Decamethylosmocene and Decamethylosmocenium: UV and X-ray Photoelectron, Magnetic, and Electronic Studies. Crystal and Molecular Structure of $[Os(C_5Me_5)_2]^{\cdot+}[BF_4]^-$

Dermot O'Hare,[1a] Jennifer C. Green,*[1b] Timothy P. Chadwick,[1b] and Joel S. Miller*[1a]

Central Research and Development Department, E. I. du Pont de Nemours and Co., Inc.,† Experimental Station E328, Wilmington, Delaware 19898, and Inorganic Chemistry Laboratory, University of Oxford, South Parks Road, Oxford OX1 3QR, U.K.

Received October 16, 1987

The complex $[Os(C_5Me_5)_2]^{\cdot+}[BF_4]^-$ has been synthesized from $Os(C_5Me_5)_2$ by oxidation with $AgBF_4$. $Os(C_5Me_5)_2$ exhibits a reversible one-electron oxidation at +0.27 vs SCE by cyclic voltammetry. Solid-state ^{13}C CPMAS NMR experiments show an axial powder symmetry indicating fast ring rotation at room temperature. The first ionization potential of $Os(C_5Me_5)_2$ is 6.68 eV as measured by photoelectron spectroscopy. Like ferrocenes, $[Os(C_5Me_5)_2]^{\cdot+}$ has a $^2E_{5/2}$ ground-state electronic structure. EPR experiments on $[Os(C_5Me_5)_2]^{\cdot+}$ at 5.2 K show axial symmetry with $g_\parallel = 5.27$, $g_\perp = 1.99$, and $\langle g \rangle = 3.08$. Solid-state and solution magnetic susceptibility data obey the Curie–Weiss expression with $\mu_{eff} = 2.70\ \mu_B$ and $\Theta = -0.5$ K. A single-crystal X-ray structure determination has been performed on $[Os(C_5Me_5)_2]^{\cdot+}[BF_4]^-$. This salt belongs to the monoclinic $C2/m$ space group [$a = 14.797$ (9) Å, $b = 8.705$ (9) Å, $c = 8.757$ (6) Å, $\beta = 109.54$ (6)°, $V = 1063$ (3) Å^3, $Z = 2$, ρ(calcd) = 1.71 g cm^{-3}]. The Os–C_5 ring centroid distance is 1.70 (4) Å, and the average Os–C, C–C, and C–Me distances are 2.02, 1.37, and 1.57 Å, respectively. The $[BF_4]^-$ anion is disordered. The charge-transfer salt $[Os(C_5Me_5)_2][C_6(CN)_6]$ has been prepared by reaction of $Os(C_5Me_5)_2$ with $[NBu_4]^+[C_6(CN)_6]^{\cdot-}$ in CH_3NO_2 and characterized as a diamagnetic material by solid-state ^{13}C NMR, EPR, and solid-state magnetic susceptibility measurement.

Introduction

One-dimensional, (1-D) charge-transfer complexes have been shown frequently to exhibit unusual optical and electrical properties.[2-4] Recently we have reported the occurrence of unusual cooperative magnetic properties for several alternating donor/acceptor charge-transfer complexes. Metamagnetic behavior, i.e., field-dependent switching from an antiferromagnetic ground state to a high moment excited state, was observed[5a] for the 1-D phase $[Fe(C_5Me_5)_2]^+[TCNQ]^{\cdot-}$[5] [TCNQ = 7,7,8,8-tetracyano-*p*-quinodimethane]; however, the tetracyanoethylenide[6,7] and hexacyanobutadienide[8] salts of $[Fe(C_5Me_5)_2]^{\cdot+}$ salts have been shown to exhibit ferromagnetic behavior. The former charge-transfer complex possesses a spontaneous magnetic moment at zero applied field.[9]

With our observation of meta- and ferromagnetic behavior in 1-D molecular charge-transfer complexes and the theoretical encouragement initially supplied by McConnell[10] that charge-transfer complexes of this structure type possessing either cations or anions with an accessible triplet (e^2) state may stabilize ferromagnetic coupling, we are continuing to prepare new materials exhibiting ferromagnetic coupling. Thus, we have undertaken the systematic study of the structure-function relationship between salts primarily comprised of metallocenium and bis(arene) cations and planar polycyanoanions with the goal of elucidating the electronic and steric requirements for the stabilization of the ferromagnetic state in a molecular material. As part of these studies we sought to prepare $[M^{III}(C_5Me_5)_2]^{\cdot+}$ (M = Ru, Os) salts for direct comparison to the highly magnetic $[Fe^{III}(C_5Me_5)_2]^{\cdot+}$-based charge-transfer complexes.

For a d^5 metallocene the electronic ground state is very sensitive to the combination of metal and ligand orbitals. Of the three possible configurations (Figure 1), the $^2A_{1g}$ is adopted by all the bis(arene)metal complexes,[11] while $[Fe(C_5H_5)_2]^{\cdot+}$, $[Fe(C_5Me_5)_2]^{\cdot+}$, and $Mn(C_5Me_5)_2$ adopt $^2E_{2g}$ ground states.[12] In contrast, $Mn(C_5H_5)_2$ may be switched from an $^2E_{2g}$ to an $^6A_{1g}$ state by a change of host material or exhibit an equilibrium between them.[13] The gas-phase ultraviolet photoelectron spectra of osmocene show that $[Os(C_5H_5)_2]^{\cdot+}$ also possesses the $^2E_{5/2'}$ ground state with the $^2A_{1/2'}$ state lying 0.41 eV above it.[14] Rhenocene has been characterized at low temperatures by photolysis of $Re(C_5H_5)_2H$ in CO or N_2 matrices at ca. 20 K.[15] This was shown to have an $^2E_{5/2'}$ ground state by magnetic circular

† Contribution No. 4559.

(1) (a) DuPont Co. (b) Oxford University.

(2) For detailed overview, see the proceedings of the recent series of international conferences: (a) *Mol. Cryst. Liq. Cryst.* **1985**, 117–121 (Pecile, C.; Zerbi, G.; Bozio, R., Girlando, A., Eds.); (b) *J. Phys., Colloq.* **1983**, 44-C3 (Comes, R., Bernier, P., Andre, J. J., Rouxel, J., Eds); (c) *Mol. Cryst. Liq. Cryst.* **1981**, 77, 79, 82, 83, 85, and **1982**, 86 (Epstein, A. J., Conwell, E. M., Eds.); (d) *Chem. Scr.* **1981**, 17 (Carneiro, K., Ed.); (e) *Lect. Notes Phys.* **1979**, 95, 96 (Bartsic, S., Bjelis, A., Cooper, J. R., Leontic, B. A., Eds.); (f) *Ann. N.Y. Acad. Sci.* **1978**, 313 (Miller, J. S., Epstein, A. J., Eds).

(3) Epstein, A. J.; Miller, J. S. *Sci. Am.* **1979**, *240*(4), 52–61. Bechgaard, K.; Jerome, D. *Sci. Am.* **1983**, *247*(2), 52–61.

(4) See, for example: Miller, J. S., Ed. *Extended Linear Chain Compounds*; Plenum: New York, 1900; Vols. 1–3. Simon, J.; Andre, J. J. *Molecular Semiconductors*; Springer-Verlag: New York, 1985.

(5) (a) Candela, G. A.; Swartzendruber, L.; Miller, J. S.; Rice, M. J. *J. Am. Chem. Soc.* **1979**, *101*, 2755–2756. (b) Miller, J. S.; Zhang, J. H.; Reiff, W. M.; Dixon, D. A.; Preston, L. D.; Reis, A. H., Jr.; Gebert, E.; Extine, M.; Troup, J.; Epstein, A. J.; Ward, M. D. *J. Phys. Chem.* **1987**, *91*, 4344.

(6) Miller, J. S.; Calabrese, J. C.; Bigelow, R. W.; Epstein, A. J..; Zhang, R. W.; Reiff, W. M. *J. Chem. Soc., Chem. Commun.* **1986**, 1026–1028.

(7) Miller, J. S.; Calabrese, J. C.; Rommelmann, H.; Chittapeddi, S. R.; Zhang, J. H.; Reiff, W. M.; Epstein, A. J. *J. Am. Chem. Soc.* **1987**, *109*, 769–781.

(8) Miller, J. S.; Zhang, J. H.; Reiff, W. M. *J. Am. Chem. Soc.* **1987**, *109*, 4584–4590.

(9) Chittapeddi, S.; Cromack, K. R.; Miller, J. S.; Epstein, A. J. *Phys. Rev. Lett.* **1987**, *22*, 2695–2698.

(10) Miller, J. S.; Epstein, A. J. *J. Am. Chem. Soc.* **1987**, *109*, 3850–3855.

(11) Cloke, F. G. N.; Dix, A. N.; Green, J. C.; Perutz, R. N.; Seddon, E. A. *Organometallics* **1983**, *2*, 1150.

(12) Smart, J. C.; Robbins, J. L. *J. Am. Chem. Soc.* **1978**, *100*, 3936.

(13) Ammeter, J. H.; Bucher, R.; Oswald, N. *J. Am. Chem. Soc.* **1974**, *96*, 7833.

(14) Cooper, G.; Green, J. C., unpublished work.

(15) Chetwynd-Talbot, D. P.; Grebenik, P.; Perutz, R. N.; Powell, M. H. A. *Inorg. Chem.* **1983**, *22*, 1675.

0276-7333/88/2307-1335$01.50/0

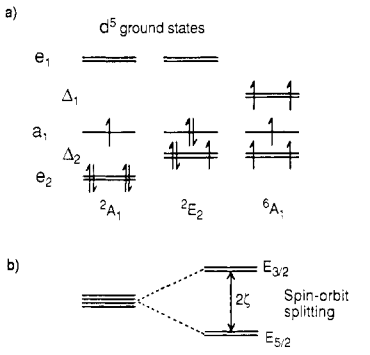

Figure 1. Three possible ground state electron configurations and terms available to d^5 parallel sandwich complexes.

dichroism. Decamethylrhenocene has recently been synthesized by co-condensation of rhenium atoms with C_5Me_5H.[16] The electronic structure has been extensively studied and indicates that the $^2E_{5/2'}$ and $^2A_{1/2'}$ states are close in energy, and population of both states occurs at temperatures close to room temperature.[17] Herein we report the results of a study on the electronic, magnetic, and structural properties of $Os(C_5Me_5)_2$ and $[Os(C_5Me_5)_2]^{+}$ and compare them to the related iron and ruthenium compounds.

Experimental Section

All reactions were performed by using standard Schlenk techniques or in a Vacuum Atmospheres Dri-Box under a nitrogen atmosphere. ^{13}C cross polarization magic angle spinning (CPMAS) spectra were obtained on a Bruker CXP-300 spectrometer (75.5 MHz). Dry nitrogen gas was used to drive the magic angle spinning (MAS) at rates of 2 kHz. Both cross-polarization (5 ms) and ^1H decoupling (40 ms) were performed at the same proton-decoupling amplitude ($\gamma(H_2)$ = 63 kHz). Chemical shifts are reported relative to $SiMe_4$ by using an external standard sample of adamantane as reference.

X-ray photoelectron spectra were measured on a Kratos ES300 X-ray photoelectron spectrometer using Mg excitation and an analyzer resolution of 0.85 eV. All compounds were pressed into an indium foil under an inert atmosphere of nitrogen in a glovebag. For $Os(C_5Me_5)_2$ the sample was maintained at −100 °C to prevent sublimation. The spectrum binding energy scale was previously calibrated to the Ag $3d_{5/2}$ peak of Ag metal at 368.3 eV.

The photoelectron spectrum was obtained by using a PES Laboratories 0078 spectrometer interfaced with a 380Z microprocessor which enabled digital collection of the data. Spectra were obtained by using both He I and He II radiation and were calibrated with reference to Xe, N_2, and He. EPR spectra were recorded on an IBM/Bruker ER 200 D-SRC spectrometer. Magnetic susceptibility data were recorded by using the Faraday technique from 3 to 300 K. Elemental analysis and single-crystal X-ray studies were performed by Oneida Research Services, Inc., Whitesboro, NY.

$Os(C_5Me_5)_2$ (1) was prepared on a 1–2-g scale according to a literature route.[18] Typically, pentamethylcyclopentadiene (Aldrich) (2.15 g, 15.9 mmol) was added to $Na_2[OsCl_6]\cdot 6H_2O$ (Alfa) (2.2 g, 3.9 mmol) in ethanol (75 mL). The mixture was refluxed for 3–4 h prior to filtering while hot. After the solution was cooled to −20 °C overnight, colorless needles were obtained. An analytically pure material was prepared by sublimation of the crystals at 10^{-3} Torr and 120 °C (yield 1.1 g, 2.3 mmol, 60%).

$[Os(C_5Me_5)_2]^{+}[BF_4]^{-}$ (2) was prepared by the addition of a solution of $Os(C_5Me_5)_2$ (100 mg, 0.21 mmol) in CH_2Cl_2 to $AgBF_4$ (40 mg, 0.20 mmol) in 5 mL of CH_3CN. A gray precipitate and a green solution were immediately formed. The solution was filtered and the solvent was removed under reduced pressure. The resulting orange solid was washed with diethyl ether (2 × 20 mL) and redissolved in CH_2Cl_2 (10 mL). Analytically pure material could be obtained by slow diffusion of diethyl ether (20 mL) into this solution (yield 100 mg, 0.18 mmol, 90%). Elemental anal. Calcd for $C_{20}H_{30}BF_4Os$: C, 43.88; H, 5.52. Found: C, 43.78; H, 5.45.

$[Os(C_5Me_5)_2][C_6(CN)_6]$ (3) was prepared by addition of a solution of $Os(C_5Me_5)_2$ (50 mg, 0.10 mmol) in CH_3NO_2 to a solution of $[NBu_4]^{+}[C_6(CN)_6]^{\bullet -}$[19] (100 mg, 0.21 mmol) in CH_3NO_2. The solution turned green, but a precipitate was not formed. The solution was concentrated to ca. 5 mL and cooled to −20 °C for 2–3 days giving bright red crystals. The red crystals were collected, washed with glyme (2 × 10 mL), and dried in vacuo (yield 48 mg, 0.07 mmol, 70%). Elemental anal. Calcd for $C_{32}H_{30}N_6Os$: C, 55.80; N, 12.20; H, 4.39. Found: C, 55.70; N, 12.05; H, 4.46. Infrared spectra (Nujol): ν(CN) 2181, 2163 cm^{-1}. These values are characteristic of $[C_6(CN)_6]^{2-}$.[19]

X-ray Data Collection for $[Os(C_5Me_5)_2]^{+}[BF_4]^{-}$ (2). Crystals of **2** were grown by slow diffusion of diethyl ether into a methylene chloride solution over 24 h. Although the crystal quality was poor, attempts to prepare better quality crystals failed. Crystallographic details for obtaining the structure of **2** are presented in Table I. A gold reflecting crystal of approximate dimensions 0.18 × 0.16 × 0.08 mm was mounted in a glass capillary in a random orientation. Preliminary examination and data collection were performed with Mo Kα radiation (λ = 0.710 73 Å) on an Enraf-Nonius CAD4 computer-controlled κ axis diffractometer.

Cell constants and an orientation matrix for the data collection were obtained from least-squares refinement using the angles of 13 reflections in the range $4 < \theta < 12°$. Systematic absences and subsequent least-squares refinement determined the space group to be $C2/m$. During data collection the intensity of three representative reflections was measured as a check on crystal stability. There was an intensity loss during data collection, and an isotropic decay correction was applied. The correction factors on I ranged from 0.930 to 1.083. Equivalent reflections were merged, and only those for which $(F_o)^2 > 2\sigma(F_o)^2$ were included in the refinement where $\sigma(F_o)^2$ is the standard deviation based on counting statistics. Data were also corrected for Lorentz and polarization factors. An empirical absorption correction with an average transmission value of 0.352 was applied.

Structure Solution and Refinement. The structure was solved by using the Patterson heavy-atom method that revealed the position of the osmium at the origin. The remaining atoms

Table I. Crystallographic Details for $[Os(C_5Me_5)_2]^{+}[BF_4]^{-}$

formula	$C_{20}H_{30}BF_4Os$
formula mass, daltons	547.47
space group	$C2/m$
a, Å	14.797 (9)
b, Å	8.705 (9)
c, Å	8.757 (6)
β, deg	109.54 (6)
V, Å^3	1063 (3)
Z	2
ρ(calcd), g cm^{-3}	1.71
cryst dimens, mm	0.18 × 0.16 × 0.08
μ(Mo Kα), cm^{-1}	60.4
F(000)	534
temp, °C	23
scan mode	ω–θ
$2\theta_{max}$, deg	56.0
total data measd	2546
unique data	1105
unique data with $(F_o)^2 > 2\sigma(F_o)^2$	323
final no. of variables	48
weighting scheme	$4(F_o)^2/\sigma^2(F_o^2)$
R_u[a]	0.085
R_w[b]	0.083
largest residual, e Å^{-3}	1.37

[a] $R_u = \sum(|F_o| - |F_c|)/\sum(|F_o|)$. [b] $R_w = \sum w(|F_o| - |F_c|)^2/\sum w(|F_o|)^2$.

(16) Cloke, F. G. N.; Day, J. P. *J. Chem. Soc., Chem. Commun.* **1985**, 967.
(17) Cooper, G.; Green, J. C., unpublished work.
(18) (a) Liles, D. C.; Shaver, A.; Singleton, E.; Wiege, M. B. *J. Organomet. Chem.* **1985**, *286*, C33. (b) Albers, M. O.; Liles, D. C.; Robinson, D. J.; Shaver, A.; Singleton, E.; Wiege, M. B.; Boeyens, J. C. A.; Levendis, D. C. *Organometallics* **1986**, *5*, 2321.
(19) Fukanaga, T. *J. Am. Chem. Soc.* **1976**, *98*, 610.

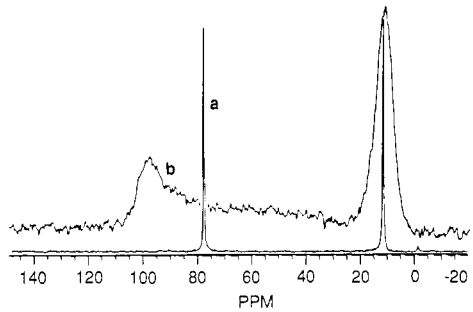

Figure 2. Solid-state state ^{13}C CPMAS spectrum of $Os(C_5Me_5)_2$ at room temperature: (a) spinning at 2 kHz; (b) nonspinning.

Table II. Summary of Chemical Shift Tensors for the Ring Carbons in the Group VIII Decamethylmetallocenes, $M(C_5R_5)_2$ (R = H, Me)

compd[a]	σ_{11}	σ_{22}	σ_{33}	$\Delta\sigma^b$	δ(sol)	ref
$Fe(C_5Me_5)_2$	101	101	34	−67	78	41
$Ru(C_5Me_5)_2$	106	106	38	−68	77	this work
$Os(C_5Me_5)_2$	98	98	35	−63	82	this work
$Mg(C_5H_5)_2$	152	152	20	−132	108	41

[a] Since $\sigma_{11} = \sigma_{22}$, we assume that the fast rotation of the substituent ring is present, causing the tensors to be axially symmetric. [b] $\Delta\sigma = \sigma_{33} - \{\sigma_{11} + \sigma_{22}\}/2$.

were located in succeeding difference Fourier syntheses. Boron was located at ($^1/_2$, 0, $^1/_2$) with site symmetry of $2/m$. There is a 2-fold disorder of the three unique F atoms about this position generating a pair of overlapping tetrahedral $[BF_4]^-$ anions. C(1) that lies in the mirror plane was located slightly out of the plane of the C_5Me_5 ring and thus was fixed at an idealized geometry. The other atoms were refined. All non-hydrogen atoms were refined with anisotropic thermal parameters in full-matrix least squares. Hydrogen atoms were not added to the structure. The final difference Fourier map showed the largest peak of 1.37 e/Å^3 near the $[BF_4]^-$ anion. Refinement converging at $R_u = 0.085$ and $R_w = 0.083$.

Neutral atom scattering factors were taken from Cromer and Weber.[20] Anomalous dispersion effects were included in F_c;[21] the values for f' and f'' were those of Cromer.[22] All calculations were performed om a VAX-11/750 computer using the SDP-PLUS package.

Results and Discussion

Recently a convenient synthesis of $Os(C_5Me_5)_2$ (1) was reported by Singleton and co-workers.[18] The compound is a white crystalline material and can be prepared on a multigram scale. However, we have found that a 1–2-g scale per reaction give the optimum yields.

Solid-State NMR of $Os(C_5Me_5)_2$ (1). The room-temperature ^{13}C cross polarization magic angle spinning (CPMAS) NMR spectrum of 1 exhibits two sharp narrow lines at 11.3 and 77.5 ppm (Figure 2). These values are in good agreement with the values found in C_6D_6 solution {77.8 (s, C_5Me_5), 10.3 ppm (s, $C_5\mathit{Me}_5$)}. The nonspinning line shape is consistent with an axially symmetric chemical shift tensor, with approximate chemical shift tensor elements σ_{11}, σ_{22}, and σ_{33} of 98, 98, and 35 ppm, respectively (Table II).

The axial symmetry arises from rotation of the C_5Me_5 group and results in averaging of the two components of the chemical shift which are in the plane of the ring and are perpendicular to the Os–(C_5Me_5) vector. This rotation must be rapid on the ^{13}C chemical shift time scale at room temperature to result in this averaging. This would also average any chemical shift inequivalences that might exist between the η-C_5Me_5 carbons. The rotation of the C_5Me_5 groups in decamethylferrocene results in a similar averaging; in this case a line-shape analysis of the variable-temperature ^{13}C data indicates that the averaging in the slow-exchange regime occurs by jumps of $2\pi/5$ with an activation energy of 13.4 kJ/mol.[23]

From the data in Table II it is clear that shielding anisotropy is very sensitive to the nature of the ring–metal interactions. The group VIII metallocenes have almost identical shielding; however, the structurally identical $Mg(C_5Me_5)_2$, with much more ionic bonding character, has much larger shielding anisotropy. Qualitatively, the greater electron density in the ring orbitals leads to greater shielding.

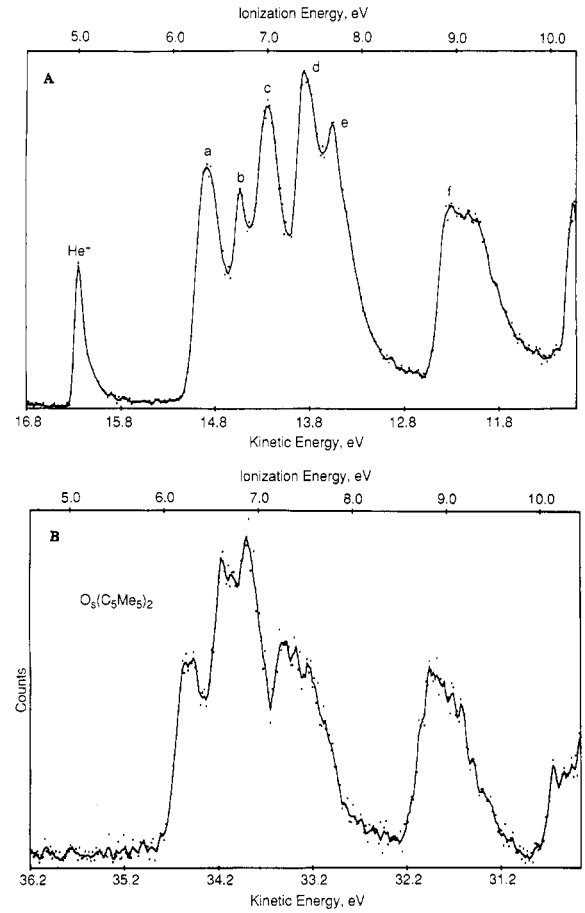

Figure 3. Low-energy region of the He I (a) He II (b) photoelectronic spectra of $Os(C_5Me_5)_2$.

Table III. Ionization Energies and Relative Intensities for the Low-Energy Region of the Photoelectron Spectrum of $Os(C_5Me_5)_2$

band	energy, eV	relative intensity[a] He I	He II	He II/He I
a	6.36	1.00	1.00	1.00
b	6.71	0.57	1.03	1.81
c	7.00	1.21	1.23	1.02
d	7.39	1.26	0.70	0.56
e	7.70	1.04	0.84	0.81
f	8.94	1.64	1.67	1.02

[a] All intensity data given relative to the first band.

(20) Cromer, D. T.; Waber, J. T. *International Tables for X-Ray Crystallography*; Kynoch: Birmingham, England, 1974; Vol. IV, Table 2.2B.
(21) Ibers, J. A.; Hamilton, W. C. *Acta Crystallogr.* **1964**, *17*, 781.
(22) Cromer, D. T.; Waber, J. T. *International Tables for X-Ray Crystallography*; Kynoch: Birmingham, England, 1974; Vol. IV, Table 2.3.1.

(23) Weimmer, D. E.; Pines, A. *J. Am. Chem. Soc.* **1981**, *103*, 34.

Table IV. Vertical Ionization Energies[a] for the Group VIII Metallocenes

compd	ion state $^2E_{2g}$	$^2A_{1g}$	$^2E_{1u}$	$^2E_{1g}$	ref
$Fe(C_5H_5)_2$	6.86	7.21	8.77	9.28	25
$Fe(C_5H_4Me)_2$	6.72	7.06	8.53	9.17	25
$Fe(C_5Me_5)_2$	5.88	6.28	7.31	8.08	24
$Ru(C_5H_5)_2$	7.45[c]	7.68	8.47	9.94	25
$Ru(C_5H_4Me)_2$	[7.25][b]	[7.25]	8.24	9.76	25
$Ru(C_5Me_5)_2$	[6.74]	[6.74]	7.34	8.95	*d*
$Os(C_5H_5)_2$	7.49[c]	7.56	8.65	10.13	42
$Os(C_5H_4Me)_2$	7.24[c]	7.21	8.26	9.9	25
$Os(C_5Me_5)_2$	6.68[a]	6.71	7.39	8.94	*d*

[a] All data accurate to 0.10 eV. [b] Numbers in square brackets are from overlapping bands. [c] Average energy of spin-orbit components. [d] Data from this work.

Ultraviolet Photoelectron Spectra of $Os(C_5Me_5)_2$. This photoelectron spectra of the metallocenes have been fully discussed.[24] The low ionization energy regions of the He I and He II spectra of decamethylosmocene are shown in Figure 3. Six maxima are discernible as observed for 1,1-dimethylosmocene.[25] The first three bands (a, b, and c) are assigned to the ionization of MO's largely composed of osmium 5d atomic orbitals. This can be justified by noting the relatively high He II/He I intensity ratios for these bands in Table III compared to bands d and e. These three maxima are thus attributable to the two ion states $^2E_2$ and $^2A_1$.

The observation of three, rather than just two, distinct bands is due to multiplet spin–orbit splitting of the orbitally degenerate $^2E_{2g}$ ion state. For pure d orbitals, the energy separation of the two multiplet components $^2E_{2(5/2)}$ and $^2E_{2(3/2)}$ should be 2ζ, where ζ is the one-electron spin–orbit coupling constant for the metal d shell. The $^2E_{2(5/2)}$ state should have the lower energy. The theoretical spin–orbit coupling constant for a free osmium monocation is 395 meV,[26] and an interpolation of the semiempirical data given by Griffith[27] suggests a value of ζ of ca. 330–430 meV. The value of ζ for osmium where the d atomic orbitals are involved in bonding will be lower than the free ion value due to the formation of molecular orbitals, leading to the effective delocalization of the originally metal d orbitals. Nevertheless, the e_2 orbitals of δ symmetry have been predicted[28] to be primarily of metal d character. Consequently bands a and c are assigned to $^2E_{2(5/2)}$ and $^2E_{2(3/2)}$ ion state bands, respectively, as they have a separation of 640 meV (Figure 3), thus implying a spin–orbit coupling constant ζ of 320 meV. This leaves us to assign band b to the a_1 (d) ionization. This assignment is further supported by the He II/He I intensity ratios (Table III), which show that band b increases in intensity relative to bands a and c when the ionizing radiation is changed from He I to He II. This is consistent with the a_{1g} orbital having greater metal d character than the e_2 orbital; a factor predicted by most calculations on metallocenes.[28]

The three bands (d, e, and f) are due to ionization from the ligand-based $e_1(\pi)$ and $e_{1''}(\pi)$ orbitals. The two ion states produced by these ionizations, $^2E_{1'}$ and $^2E_{1''}$, are both orbitally degenerate and are thus susceptible to Jahn–Teller splitting. This explains the observation of three bands; bands d and e are two Jahn–Teller components of the same ion state, and band f is broader than the others. As stated earlier, many calculations have shown that the $e_{1''}(\pi)$ orbital is dominant in ring–metal bonding and has some metal d character. The $e_{1'}(\pi)$ orbital is nonbonding and has effectively no d character by symmetry. Band f has considerably a greater He II/He I ratio than bands d and e. This is consistent with the assignment of band f with the $^2E_{1''}$ ion state and bands d and e with the $^2E'_1$ ion state. Thus, ordering of the ion states for $[Os(C_5Me_5)_2]^{+}$ is $^2E_{2(5/2)'} > {}^2A_1' > {}^2E_{2(3/2)'} > {}^2E > {}_{1'} > {}^2E_{1''}$.

As shown in Table IV on descending group VIII metallocenes there is a gradual increase in the first ionization potential; this is also reflected in the increase of the electrochemical oxidation potential for the $[M]^{2+}/[M]^{3+}$ couple. For a particular element, the addition of methyl substitution increases the electron density at the metal center and lowers the first ionization potential. Empirically the lowering of the ionization potential is ~0.1 eV per methyl group.

Synthesis and Characterization of $[Os(C_5Me_5)_2]^{+}[BF_4]^-$ (2). Oxidation reactions of 1 with halogens and protonation reactions were reported by Singleton and co-workers;[18] however, the synthesis of the 17-electron cation $[Os(C_5Me_5]_2^{+}$ was not reported. Cyclic voltammetry shows that $Os(C_5Me_5)_2$ exhibits an reversible redox couple at 0.46 V (vs SCE) with $\Delta(E_a - E_c) = 140$ mV (at 100 mV/s) and $i_a/i_c = 1.0$ in CH_2Cl_2. Bulk coulometry experiments show that the redox couple is an one-electron process and that the oxidized species is stable in CH_2Cl_2 solution. Like $Fe(C_5Me_5)_2$, $Os(C_5Me_5)_2$ can be chemically oxidized to the stable 17-electron radical $[Os(C_5Me_5)_2]^{+}[BF_4]^-$ (2) with $AgBF_4$. Gold reflecting crystals of 2 can be obtained by crystallization from methylene chloride/diethyl ether solution. This is in contrast to $[Ru(C_5Me_5)_2]^{+}$ which is very unstable in solution and decomposes within minutes at room temperature at CH_2Cl_2 to the diamagnetic compound $[Ru(C_5Me_5)(\eta^6\text{-}C_5Me_4CH_2)]^+$.[29] In addition there is a slight drop in $E_{1/2}$ from 0.55 V (vs SCE) for $Ru(C_5Me_5)_2$ to 0.46 V for $Os(C_5Me_5)_2$. This is consistent with the adiabatic ionization

Table V. Bond Distances (Å) for $[Os(C_5Me_5)_2]^{+}[BF_4]^-$ (2)

Os(1)–C(1)	1.977	C(2)–C(12)	1.61 (6)
Os(1)–C(2)	2.03 (4)	C(3)–C(3)	1.37 (4)
Os(1)–C(3)	2.08 (3)	C(3)–C(13)	1.57 (5)
C(1)–C(2)	1.41 (3)	F(1)–B(1)	1.44 (7)
C(1)–C(11)	1.538	F(2)–B(1)	1.51 (6)
C(2)–C(3)	1.34 (4)	F(3)–B(1)	1.28 (5)

Tablle VI. Bond Angles (deg) for $[Os(C_5Me_5)_2]^{+}[BF_4]^-$ (2)[a]

C(2)–C(1)–C(2)	113.0 (20)	C(3)–C(3)–C(12)	130.0 (30)
C(2)–C(1)–C(11)	124.0 (10)	C(2)–C(3)–C(3)	112.0 (30)
C(1)–C(2)–C(3)	101.0 (20)	C(2)–C(3)–C(13)	123.0 (30)
C(1)–C(2)–C(12)	126.0 (30)	C(3)–C(3)–C(13)	125.0 (30)

[a] Numbers in parentheses are estimated standard deviations in the least significant digits.

(24) (a) Turner, D. W. *Physical Methods on Advanced Inorganic Chemistry*; Hill, H. A. O, Day, P., Eds.; Interscience: New York, 1968. (b) Rabalais, J. W.; Werne, L. O.; Bergmark, T.; Karlsson, L.; Hussain, M.; Siegbain, K. *J. Chem. Phys.* **1972**, *57*, 1185. (c) Evans, S.; Green, M. L. H.; Jewitt, B.; King, G. H.; Orchard, A. F. *J. Chem. Soc., Faraday Trans. 2*, **1974**, *70*, 356. (d) Cauletti, C.; Green, J. C.; Kelly, M. R.; Robbins, J. L.; Smart, J. C. *J. Electron Spectrosc. Relat. Phenom.* **1980**, *19*, 327.

(25) Evans, S.; Green, M. L. H.; Jewitt, B.; Orchard, A. F.; Pygall, C. F. *J. Chem. Soc., Faraday Trans. 2* **1972**, *68*, 1847.

(26) Fraga, S.; Karwowski, J.; Saxena, K. M. S. *Handbook of Atomic Data*; Elsevier: New York, 1976.

(27) Griffith, J. S. *The Theory of Transition Metal Ions*; CUP: London, 1961.

(28) (a) Warren, K. D. *Struct. Bonding (Berlin)* **1981**, *27*, 45. (b) Botrel, A.; Dibout, P.; Lissillows, R. *Theor. Chim. Acta* **1975**, *37*, 37. (c) Bagus, P. S.; Walgren, U. I.; Almlof, J. *J. Chem. Phys.* **1976**, *64*, 2324. (d) Clack, D. W. *Theor. Chim. Acta* **1974**, *35*, 157.

(29) (a) Kolle, U.; Grub, J. *J. Organomet. Chem.* **1983**, *243*, C27 (b) Kolle, U.; Grub, J. *J. Organomet. Chem.* **1985**, *289*, 133.

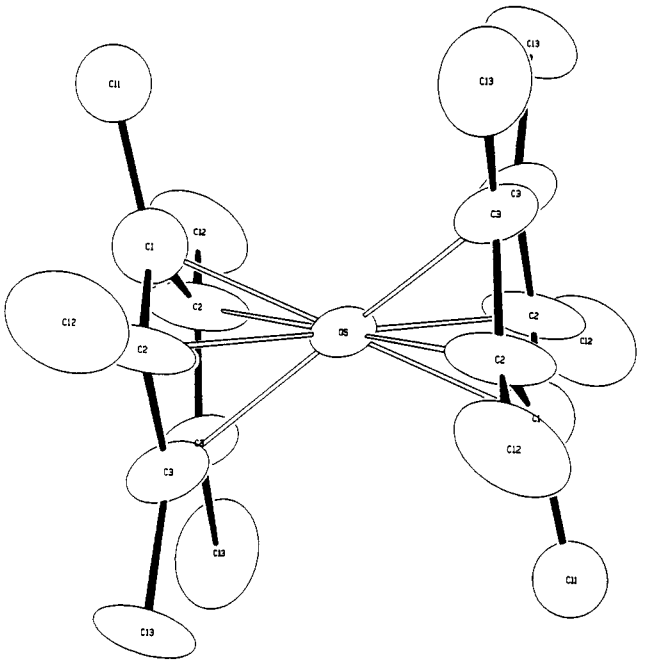

Figure 4. Molecular structure of $[Os(C_5Me_5)_2]^{\bullet+}[BF_4]^-$ showing labeling scheme.

Table VII. Positional Parameters[a] for $[Os(C_5Me_5)_2]^{\bullet+}[BF_4]^-$ (2)

atom	x	y	z	B,[b] Å²
Os(1)	0.000	0.000	0.000	5.49 (8)
C(1)	−0.105	0.000	0.093	8.0[c]
C(2)	−0.111 (3)	0.135 (4)	0.001 (3)	9 (1)
C(3)	−0.133 (2)	−0.078 (3)	−0.148 (3)	7 (1)
C(11)	−0.090	0.000	0.275	8.0*
C(12)	−0.120 (3)	0.308 (6)	0.061 (5)	15 (2)
C(13)	−0.166 (3)	0.182 (6)	−0.304 (4)	18 (2)
F(1)	0.532 (5)	0.000	0.362 (7)	11.9[c]
F(2)	0.397 (5)	0.000	0.389 (8)	13.7*
F(3)	0.036 (3)	−0.366 (6)	0.504 (7)	17.0[c]
B(1)	0.500	0.000	0.500	10.0[c]

[a] Estimated standard deviations in parentheses. [b] Anisotropically refined atoms are given in the form of the isotropic equivalent displacement parameter defined as $(^4/_3)[a^2B(1,1) + b^2B(2,2) + c^2B(3,3) + ab(\cos\gamma)B(1,2) + ac(\cos\beta)B(1,3) + bc(\cos\alpha)B(2,3)]$. [c] Atoms with an asterisk were refined isotropically.

energy of 6.1 and 6.4 eV for $Os(C_5Me_5)_2$ and $Ru(C_5Me_5)_2$, respectively.

Recently, oxidation of $Os(C_5H_5)_2$ to the metal–metal bonded dimer dication has been reported.[30] The analogous structure has been observed for $Re(C_5H_5)_2$;[31] however, permethylosmocene does not undergo dimerization presumable due to steric constraints.

X-ray Structure Determination. Compound **2** crystallizes in the monoclinic space group $C2/m$. The atom labeling for $[Os(C_5Me_5)_2]^{\bullet+}$ is shown in Figure 4, and the bond distances and angles are given in Tables V and VI, respectively. Tables of positional coordinates and thermal parameters are found in Tables VII and S1, respectively. The X-ray structure confirms that **2** is monomeric and is not the dimer dication. The cyclopentadienyl rings adopt a D_{5d} staggered conformation in the solid state. A staggered conformation of the C_5Me_5 groups has also been found for decamethylferrocene,[32] and it has been calculated

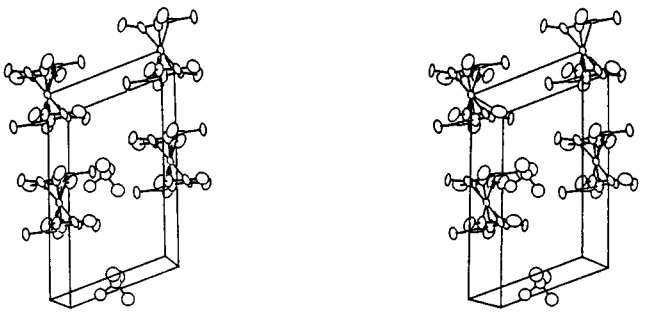

Figure 5. Stereoview of $[Os(C_5Me_5)_2]^{\bullet+}[BF_4]^-$.

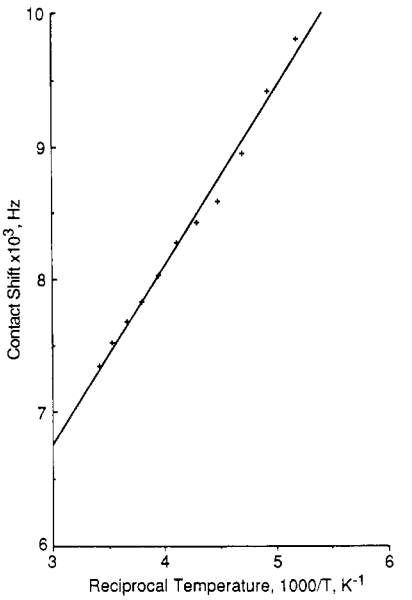

Figure 6. Plot of ^1H contact shift ($\Delta\nu$) vs T^{-1} for $[Os(C_5Me_5)_2]^{\bullet+}[BF_4]^-$ in CD_2Cl_2.

that this form is 4.2 kJ mol^{-1} more stable than the eclipsed form.[33] However, for both decamethylruthenocene[18] and decamethylosmocene[18] only the eclipsed forms have been observed. The greater separation of the cyclopentadienyl rings (interplanar distance of 3.60 and 3.61 Å, respectively, compared to 3.31 Å for decamethylferrocene) can accommodate the eclipsed conformation with less steric interactions. However, for **2** the interplanar separation of 3.40 Å for the C_5Me_5 rings dictates a staggered conformation to prevent unfavorable methyl–methyl contacts.

A stereoview of the unit cell for **2** is shown in Figure 5. The cations and anions stack in segregated chains and the $[Os(C_5Me_5)_2]^{\bullet+}$ cations within a chain align so that their principal axes are parallel with alternate cations being displaced by $b/2$.

Magnetic Properties. Paramagnetic NMR Studies. Solutions of **2** in CD_2Cl_2 exhibit a contact shifted ^1H resonance at 22.5 ppm [$\Delta\nu$ = 6.75 kHz, relative to $Os(C_5Me_5)_2$ with a line width at half-height, $\omega_{1/2}$, of 750 Hz at room temperature]. Both the contact shift and line width vary linearly with reciprocal temperature between 180 and 300 K (Figure 6). This is strong evidence that **2** is stable in solution and ligand dissociation is not occurring.

Under the conditions of rapid electron relaxation, when the Curie law is obeyed, the nuclear magnetic resonance contact shift $\delta\nu$ (Hz) is given by eq 1,[34] where $\Delta\nu$ = NMR

$$\frac{\Delta\nu}{\nu_0} = \frac{-A\langle g\rangle\mu_B S(S+1)}{g_N\mu_N(3k_BT)} \qquad (1)$$

(30) Droege, M. W.; Harman, W. D.; Taube, H. *Inorg. Chem.* **1987**, *26*, 1309.
(31) Pasman, P.; Snel, J. J. M. *J. Organomet. Chem.* **1984**, *276*, 387.
(32) Freyberg, D. P.; Robins, J. L.; Raymond, K. N.; Smart, J. C. *J. Am. Chem. Soc.* **1979**, *101*, 892.
(33) Carter, S.; Murrel, J. N. *J. Organomet. Chem.* **1980**, *192*, 399.

Table VIII. Selected EPR Data on Some d^5 Metallocene and Bis(arene) Complexes

compd	temp, K	$g_\parallel$	$g_\perp$	$\langle g \rangle^e$	electron config	ref
$[Fe(C_5Me_5)_2]^{+}$	4[a]	4.35	1.26	2.29	$^2E_2$	49
$[Ru(C_5Me_5)_2]^{+}$	77[b]	2.06	2.00	2.02	^2E	29a
$[Os(C_5Me_5)_2]^{+}$	4[b]	5.27	1.99	3.08	$^2E_{5/2}$	this work
$Mn(C_5H_5)_2$	4[c]	very broad			$^2E_{2g} \rightleftharpoons {}^6A_{1g}$	42
$Mn(C_5H_4Me)_2$	4[c]	2.90	1.89	2.22	$^2E_{2g} \rightleftharpoons {}^6A_{1g}$	44
$Mn(C_5Me_5)_2$	12[c]	3.36	1.42	2.06	$^2E_{2'}$	43
$Re(C_5H_5)_2$	[f]	matrix species			$^2E_{5/2}$	47
$Re(C_5Me_5)_2$	4[d]	4.87	<0.34		$^2E_{5/2}$	14
$[Cr(C_6H_6)_2]^{+}$	room temp[d]	198[e]			$^2A_{1g}$	45
$V(C_6H_6)_2$	room temp[d]	198[e]			$^2A_{1g}$	46

[a] In dimethylformamide. [b] In dichloromethane. [c] Methylcyclohexane glass. [d] In toluene. [e] Isotropic signal, $\langle g \rangle = \{2g_\perp + g_\parallel\}/3$. [f] $g_\parallel = 3.35 \pm 0.37$ for magnetic circular dichroism.[48]

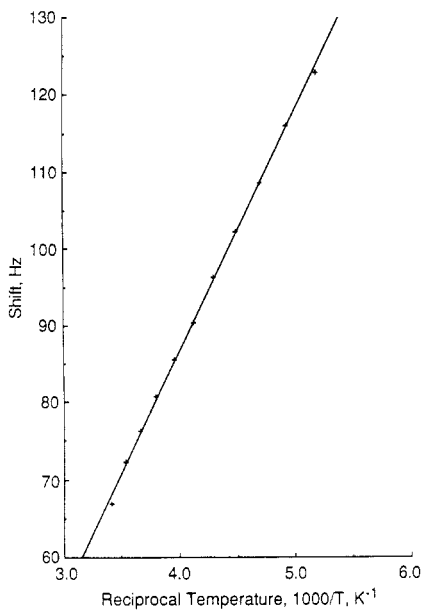

Figure 7. Plot of shift ($\Delta\nu$) vs T^{-1} for the Evans magnetic susceptibility measurement for $[Os(C_5Me_5)_2]^{+}[BF_4]^-$ in CD_2Cl_2.

contact shift (Hz), ν_0 = resonance frequency (Hz), μ_B = Bohr magneton, and μ_N = nuclear magneton, g_N = nuclear g value, $\langle g \rangle$ = isotropic electron g value, and A = electronic hyperfine coupling constant. We also note that the contact shift for $Fe(C_5Me_5)_2$ is −39 ppm which is a dramatic difference from the isostructural and presumably isoelectronic metallocene.

The magnetic moment of **2** measured in solution between 180 and 300 K using the Evans method[35] yields the isotropic value of 2.77 μ_B. This value was found to be independent of concentration (in the range (0.1–0.5) × 10^{-4} M) and magnetic field strength (250–400 MHz). For an accurate solution determination of the magnetic moment the temperature variation of the observed shift should be measured (Figure 7). For a superconducting magnetic field configuration the susceptibility is given by eq 2, where

$$\chi_m = \frac{3\delta\nu}{4\pi\nu_0 c} + \chi_o M + \chi_o \frac{(d_o - d_s)}{c} \qquad (2)$$

$\Delta\nu$ = frequency shift (Hz), ν_0 = applied field (Hz), χ_M = molar magnetic susceptibility, χ_o = solvent susceptibility, M = molecular weight, d_o = solvent density, d_S = solution density, and c = molar concentration. Thus

$$\delta\nu \propto \left(\frac{\mu^2_{eff}}{T}\right) + \text{constant}$$

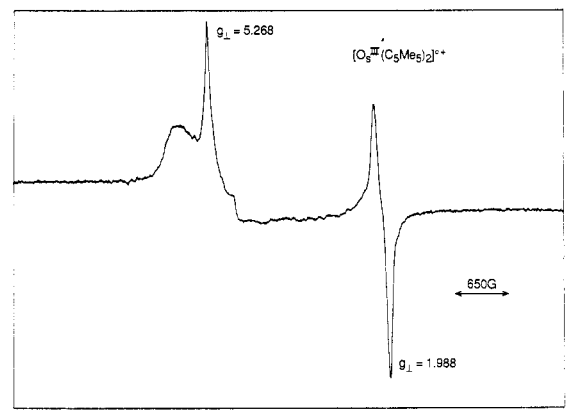

Figure 8. EPR spectra for $[Os(C_5Me_5)_2]^{+}[BF_4]^-$ in CD_2Cl_2 at 5.4 K.

Table IX. Comparison of Physical Properties of $[M(C_5Me_5)_2]^{+}$ (M = Fe, Ru, Os)

property	$[Fe(C_5Me_5)_2]]^{+}$	$[Ru(C_5Me_5)_2)]^{+}$	$[Os(C_5Me_5)_2]^{+}$
^{1}H NMR contact shift,[a] ppm	−39		+22
^{1}H NMR line width,[a] Hz	310		720
g values ($g_\parallel$, $g_\perp$)[b]	4.35, 1.26	2.06, 2.00	5.27, 1.99
$\langle g \rangle$[c]	2.29	2.02	3.08
μ_{eff}, μ_B	2.54		2.77
1st IP, eV	5.88	[6.74]	6.68
$E_{1/2}$,[d] V	−0.12	+0.55[29b]	+0.46
d(M–C_{ring}), Å	2.09		2.02

[a] In CH_3CN. [b] Frozen solution, 4 K. [c] $\langle g \rangle = \{2g_\parallel + g_\parallel\}/3$. [d] In CH_2Cl_2 vs SCE.

For **2** the temperature-independent term leads to an error of ±15% in the single room-temperature measurement if it is ignored in the calculation of the solution susceptibility.

Electron Spin Resonance. The magnetic properties of the metallocenes have been thoroughly investigated from both an experimental and theoretical viewpoint.[36] The simplest behavior is found for systems with orbitally nondegenerate ground states, that is compounds with 15-electron $^4A_{1g}$ {$V(C_5H_5)_2$ and $[Cr(C_5H_5)_2]^{+}$} or 20-electron $^3A_{2g}$ $[Ni(C_5H_5)_2]$ configurations. Orbital contributions to the moment are not expected, and the magnetic moments are close to the spin-only value. In addition, the EPR spectra of these metallocenes can be observed at room temperature and the g and A values are insensitive to changes in host matrix.[37]

(34) (a) Anderson, S. E.; Drago, R. S. *J. Am. Chem. Soc.* **1970**, *92*, 4244. (b) Rettig, M. F.; Drago, R. S. *J. Am. Chem. Soc.* **1969**, *91*, 1361.
(35) Deutsch, J. L.; Poling, S. M. *J. Chem. Educ.* **1969**, *46*, 167.
(36) Warren, K. D. *Inorg. Chem.* **1974**, *13*, 1317. Gordon, K. R.; Warren, K. D. *Inorg. Chem.* **1978**, *17*, 987.
(37) Ammeter, J. H. *J. Magn. Reson.* **1978**, 299. Zoller, L.; Moser, E.; Ammeter, J. H. *J. Phys. Chem.* **1986**, *90*, 6632. Robbins, J. L.; Edelstein, N.; Spencer, B.; Smart, J. C. *J. Am. Chem. Soc.* **1982**, *104*, 1882.

Table X. Summary of Important XPS Binding Energy Values[a] for $[Os(C_5Me_5)_2]^n$ (n = 0, 1+, 2+)

sample	Os($4f_{7/2}$)	Os($4f_{5/2}$)	C(1s)	F(1s)	B(1s)	N(1s)
$Os(C_5Me_5)_2$	51.4 (1.7)[b]	54.1	285.8 (1.7)			
$[Os(C_5Me_5)_2][BF_4]$	52.5 (1.7)	55.1	285.5 (1.9)	686.2	194.5	
$[Os(C_5Me_5)_2][C_6(CN)_6]$	52.5 (1.8)	55.1	285.3 (2.0)			398.4

[a] Samples measured on indium. [b] Values in parentheses are peak widths at half-maximum (eV).

In contrast, low-spin 17-electron metallocenes possess degenerate $^2E_{2g}$ [e_{2g}^3, a_{1g}^2] electronic configurations. Significant orbital contributions to the magnetic moment are expected that should lead to observed moments larger than the spin-only value. The degenerate electronic configuration leads to fast electronic relaxation; thus, EPR spectra can typically only be observed at very low temperatures and the g and A parameters very host dependent (Table VIII). Compound **2** exhibits an EPR signal only at temperature ~4 K; the spectrum in frozen dichloromethane shows an axial pattern with g values of $g_\parallel = 5.27$, $> g_\perp = 1.99$, and $\langle g \rangle = 3.08$ (Figure 8). No proton hyperfine coupling is resolvable.

Magnetic Susceptibility. The solid-state magnetic susceptibility measurements on finely powdered samples of **2** showed that the compound obeyed the Curie–Weiss expression over the temperature range 2.4–300 K with $\mu_{eff} = 2.75\ \mu_B$ and $\Theta = -1.4$ K (Figure 9). The μ_{eff} is in good agreement with the EPR data since with use of eq 3 (where $\mu_\parallel^2 = S(S+1)g_\parallel^2$, $\mu_\perp^2 = S(S+1)g_\perp^2$, $g_\parallel = 5.27$, $g_\perp = 1.99$, g = Lande' g factor, μ_{eff} = effective moment, and $\langle \mu \rangle$ = isotropic moment), a value for $\mu_{eff} = 2.9\ \mu_B$ is obtained.

$$\langle \mu \rangle = [(\mu_\parallel^2 + 2\mu_\perp^2)/3]^{1/2} \quad (3)$$

The EPR results indicate that the material is highly anisotropic, and this manifests itself in the solid-state magnetic susceptibility measurements. The susceptibility of an aligned single crystal has a moment as great as 4.35 μ_B. This is close to the maximum moment of 4.55 μ_B which would correspond to alignment of all the $g_\parallel$ vectors as shown in the packing diagram (Figure 5).

A comparison of the physical properties of $[M(C_5Me_5)_2]^{\bullet+}$ (M = Fe, Ru, Os) is summarized in Table IX.

Synthesis and Characterization of $[Os(C_5Me_5)_2][C_6(CN)_6]$. Reaction of $Os(C_5Me_5)_2$ with 2 equiv of $[Bu_4N]^+[C_6(CN)_6]^{\bullet-}$ in CH_3NO_2 yields a red solution from which bright red crystals of a 1:1 salt, **3**, can be isolated. The material is insoluble in CH_2Cl_2, THF, or CH_3NO_2, and decomposition is evident upon dissolution in hot CH_3CN. The infrared spectrum shows two sharp CN stretches in the correct position and intensity ratio for the diamagnetic $[C_6(CN)_6]^{2-}$.[19,38] The salt is EPR silent, and the solid-state susceptibility shows the material to be diamagnetic in the temperature range 3–320 K. The ^{13}C CPMAS spectrum at room temperature clearly indicates the presence of η-C_5Me_5 ligands as resonances at 104.6 (C_5Me_5) and 9.8 ppm ($C_5\mathit{Me}_5$). In addition, weaker resonances at 127.8, 126.1, and 30.4 are assignable to (^{13}CN) of the $[C_6(CN)_6]^{2-}$ ligand. We have been unable to obtain X-ray structural information on this material; thus, the precise nature of this solid is still unknown. The solution electrochemistry of $Os(C_5Me_5)_2$ and $[C_6(CN)_6]^{\bullet-}$ shows that $Os(C_5Me_5)_2$ will reduce 1 equiv of $[C_6(CN)_6]^{\bullet-}$ to the diamagnetic dianion. Thus, in solution we have equimolar amounts of $[Os(C_5Me_5)_2]^{\bullet+}$, $[C_6(CN)_6]^{\bullet-}$, and $[C_6(CN)_6]^{2-}$. Solid-state crystallization energies may then favor the formation of the insoluble 1:1 phase containing $[Os(C_5Me_5)_2]^{\bullet+}[C_6(CN)_6]^{\bullet-}$ where electron transfer to form diamagnetic $[Os(C_5Me_5)_2]^{2+}[C_6(CN)_6]^{2-}$ occurs.

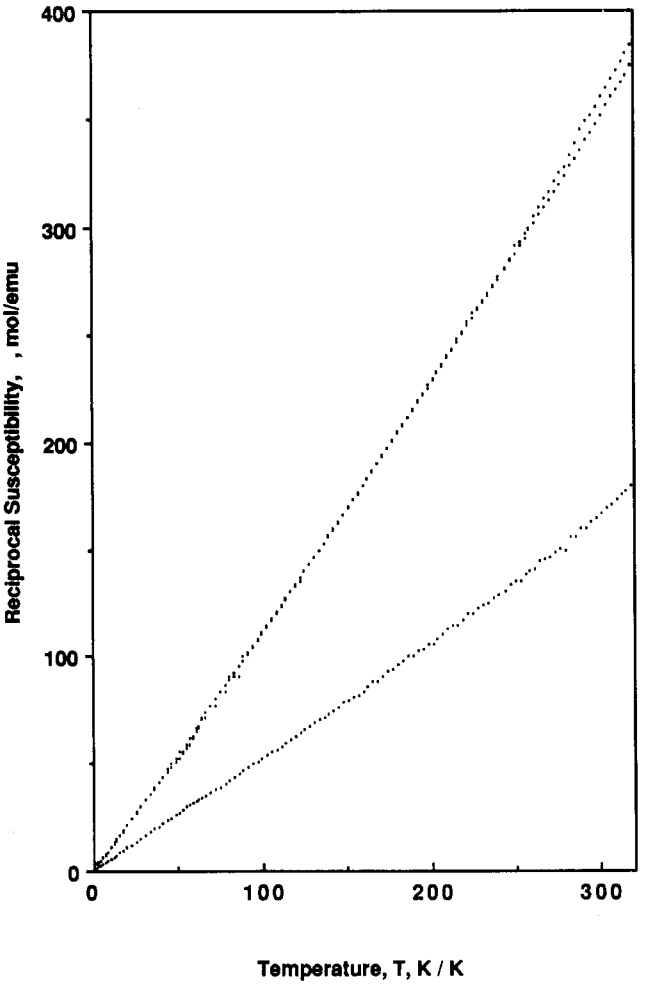

Figure 9. Plot of χ_M^{-1} vs T for $[Os(C_5Me_5)_2]^{\bullet+}[BF_4]^-$.

Other Charge-Transfer Salts. $Os(C_5Me_5)_2$ was reacted with a range of cyanocarbon acceptors in an effort to prepare complexes analogous to the $[Fe(C_5Me_5)_2]^{\bullet+}$-[anion]$^-$ complexes prepared previously and characterized to exhibit cooperative magnetic properties.[39] Reaction of $Os(C_5Me_5)_2$ with stoichiometric quantities of either TCNE (TCNE = tetracyanoethylene), TCNQ (TCNQ = 7,7,8,8-tetracyano-*p*-quinodimethane), $C_4(CN)_6$, $TCNQF_4$ ($TCNQF_4$ = perfluoro-7,7,8,8-tetracyano-*p*-quinodimethane), or DDQ (DDQ = 2,3-dichloro-5,6-dicyanobenzene) gave amorphous solids that did not yield crystals suitable for single-crystal X-ray diffraction. Elemental analysis of these solids indicated that they were generally $[Os(C_5Me_5)_2][anion]_x$ (x = 1 or 2) salts. The infrared ν(CN) bands were always broad, possibly indicating multiphase materials. However, the EPR or magnetic susceptibility data indicated that these charge-transfer solids were diamagnetic; hence within the context of seeking charge-transfer salts exhibiting cooperative magnetic properties, these compounds did not warrant further study.

(38) Dixon, D. A.; Miller, J. S. *Science (Washington, D.C.)* **1987**, *235*, 871.

(39) Miller, J. S.; Epstein, A. J.; Reiff, W. M. *Chem. Rev.* **1988**, *88*, 201.

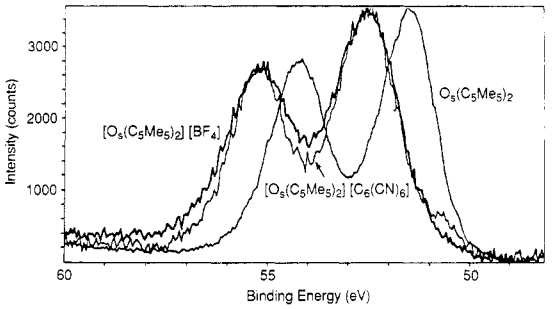

Figure 10. Part of the XPS spectra of $[Os(C_5Me_5)_2]^n$ (n = 0, 1+, 2+) showing the osmium $4f_{7/2}$ and $4f_{5/2}$ photoemission peaks.

Ru Charge-Transfer Salts. The complex $[Ru(C_5Me_5)_2]^{\bullet+}[BF_4]^-$ has been previously reported,[29a] and the EPR indicates that this radical cation shows smaller magnetic anisotropy (Table VIII) than $[M(C_5Me_5)_2]^{\bullet+}$ (M = Fe or Os), even though photoelectron spectroscopy (Table IV) and theoretical considerations conclude that $[Ru(C_5Me_5)_2]^{\bullet+}$ also has an ^2E ground state.[17] Of fundamental interest is the magnetic properties of one-dimensional charge-transfer salts based on this organometallic cation. Unfortunately our experiments have shown that $[Ru^{III}(C_5Me_5)_2]^{\bullet+}$ is very unstable in solution decomposing to the diamagnetic $[Ru^{II}(C_5Me_5)(\eta^6\text{-}C_5Me_4CH_2)]^+$ cation and $Ru^{II}(C_5Me_5)_2$ in ca. 1–2 min in CH_2Cl_2 at −25 °C and almost instantaneously in CH_3CN. The cyclic voltammetry obtained reduction potential of $Ru(C_5Me_5)_2$ is 0.55 V (vs SCE).[29b] Consequently, neither TCNQ nor TCNE is strong enough of an acceptor to oxidize $Ru(C_5Me_5)_2$. Hexacyanobutadiene is strong enough to oxidize $Ru(C_5Me_5)_2$; however, even under rapid precipitation conditions at low-temperature disproportionation dominates and crystalline charge-transfer materials could not be isolated.

X-ray Photoelectron Studies. Core binding energies of a 1, 2, and 3 were measured by XPS to assess the oxidation states of osmium in these materials, and in particular the oxidation state of osmium in compound 3. Figure 10 shows the Os $4f_{7/2}$ and $4f_{5/2}$ photoemission peaks for 1, 2, and 3. A summary of the binding energy values is found in Table X. For 1 the Os $4f_{7/2}$ and $4f_{5/2}$ peaks were found at 51.4 and 54.1 eV. These values fall midway in the range of energies found for the measured Os(II) complexes.[40] For both 2 and 3 the $4f_{7/2}$ and $4f_{5/2}$ peaks were located at 52.4 and 55.1 eV, respectively, indicating a similar charge distribution around the Os centers and in the range found for Os(III) compounds, and so we conclude from these experiments we would assign the oxidation state of osmium in 3 as Os(III). This is inconsistent with the diamagnetic properties, and resolution must await the availability of single crystals suitable for single-crystal X-ray analysis.

Acknowledgment. We wish to thank L. Firment (XPS measurements), M. Ward (electrochemistry), and D. Wipf, S. McLean, B. Carver, and W. Bachmann for their technical assistance.

Registry No. 1, 100603-32-5; 2, 113509-52-7; 3, 113509-53-8; $[NBu_4]^+[C_6(CN)_6]^-$, 58608-56-3; $Ru(C_5Me_5)_2$, 84821-53-4.

Supplementary Material Available: Tables of the least-squares planes and anisotropic thermal parameters (2 pages); a listing of calculated and observed structure factors (2 pages). Ordering information is given on any current masthead page.

(40) Lin'to, I. V.; Zaitsev, B. E.; Molodkin, A.; Ivanova, T. M.; Linko, R. V. *Russ. J. Inorg. Chem. (Engl. Transl.)* **1983**, *26*, 857.
(41) Weimmer, D. E.; Ruben, D. J.; Pines, A. *J. Am. Chem. Soc.* **1981**, *103*, 28.
(42) Cooper, G.; D. Phil. Thesis, Oxford, 1987.
(43) Robbins, J. L.; Edelstein, N. M.; Cooper, S. R.; Smart, J. C. *J. Am. Chem. Soc.* **1979**, *101*, 3853.
(44) Switzer, M. E.; Wang, R.; Rettig, M. F.; Maki, A. H. *J. Am. Chem. Soc.* **1974**, *96*, 7669.
(45) Ting-Tung, T.; Kung, W.-J.; Ward, D. L.; McCulloch, B.; Brubaker, C. H. *Organometallics* **1982**, *1*, 1229.
(46) Andrews, M. P.; Mattar, S. M.; Ozin, G. A. *J. Phys. Chem.* **1986**, *90*, 1037.
(47) Cox, P. A.; Grebenik, P.; Perutz, R. N.; Graham, R. G.; Grinter, R. *Chem. Phys. Lett.* **1984**, *108*, 415.
(48) Perutz, R. N.; Graham, R. G.; Grinter, R., unpublished work.
(49) Duggan, D. M.; Hendrickson, D. N. *Inorg. Chem.* **1975**, *14*, 955.

Electronic Structure of Piano-Stool Dimers. 5. Relationships between the π-Acidity and Electrochemistry in a Series of Isoelectronic Compounds of the Type $Cp_2M_2L_4$ (L = CO, NO)[1]

Bruce E. Bursten,*[2] Roger H. Cayton, and Michael G. Gatter

Department of Chemistry, The Ohio State University, Columbus, Ohio 43210

Received October 16, 1987

The electronic structures of a series of isoelectronic piano-stool dimers of the formulation $[CpM(EO)]_2(\mu\text{-}EO)_2$ (M = Cr, Mn, Fe; E = C, N) have been investigated via nonempirical Fenske–Hall molecular orbital calculations. The π-acid effects of CO vs NO on the frontier orbitals within this system were extracted by comparing the calculated electronic structures with the bonding in the corresponding "σ-only" frameworks, $[CpM(H)]_2(\mu\text{-}H)_2$ (M = Cr, Mn, Fe). These results were then used to explain the directly converse electrochemical results of the iron and chromium dimers. The redox chemistry of these dimers appears to be governed by the nature of the frontier orbitals. For the manganese dimer, the possibility of other geometric isomers has been investigated and predictions have been advanced concerning its yet uninvestigated electrochemistry.

Transition-metal dimers of the general formula $[CpM]_2L_n$ (Cp = $\eta^5\text{-}C_5H_5$), termed piano-stool dimers, comprise a wide class of organometallic compounds displaying a variety of structure types depending on the

0276-7333/88/2307-1342$01.50/0